

Miniaturized Ultra-Wide Band (UWB) Delta-Stub Based 4-Way Power Divider with Enhanced Isolation For Internet of Things (IoT) and Next-Generation Wireless Systems

Original Scientific Paper

Arshad Karimbu Vallappil*

Institute of Space Sciences (ICE, CSIC),
Campus UAB, Carrer de Can Magrans, s/n 08193, Cerdanyola del Vallès, Barcelona, Spain
kv.arshad@gmail.com, karimbu@ice.csic.es

Bilal A. Khawaja*

Faculty of Engineering, Department of Electrical Engineering,
Islamic University of Madinah, P. O. BOX 170 Madinah, 41411, Saudi Arabia
kjbmohammed@iu.edu.sa, bam.khawaja@gmail.com

Abdulmajeed M Alenezi

Faculty of Engineering, Department of Electrical Engineering,
Islamic University of Madinah, P. O. BOX 170 Madinah, 41411, Saudi Arabia
a.alenezi@iu.edu.sa

*Corresponding author

Abstract – This paper proposes a novel wideband 1-to-4-way Wilkinson power divider (WPD) designed for operation in the ultra-wideband (UWB) frequency band. The proposed power divider operates in the frequency range of 3-8GHz. The design process started with conventional WPD design and evolved based on three stages of a 1-to-2 way power divider, incorporating 100Ω resistors and two delta-stubs for each stage. Delta-stubs are introduced in the WPD design for enhanced operational bandwidth and impedance-matching characteristics. The proposed power divider is designed using an FR4 substrate with a thickness of 0.76mm and ϵ_r of 4.3, respectively. The proposed design exhibits equal power split at all ports, good insertion-loss of approximately -6 ± 2 dB, and return-loss of below -10 dB over the operating frequency band. Moreover, good impedance-matching, and isolation performance have been obtained over the desired frequency band. The proposed WPD was initially modeled mathematically and then designed and optimized using CST microwave studio (CST-MWS). The proposed design can be used in the next-generation UWB-Internet of Things (UWB-IoT) antenna array systems.

Keywords: UWB, Wilkinson Power Divider, Delta-Stub, Antenna Array Systems, Internet of Things (IoT)

Received: April 16, 2024; Received in revised form: July 18, 2024; Accepted: August 9, 2024

1. INTRODUCTION

The last decade has seen a significant interest in ultra-wideband (UWB) technology [1-3] due to its enhanced bandwidth, radiation characteristics, and increased data-transmission features [2-4]. The Federal Communication Commission (FCC), USA, has designated a frequency band of 3.1-10.6 GHz (7.5 GHz bandwidth) for use in UWB applications [1-3]. Both wireless systems and sensor networks benefit greatly from UWB technology's enhanced data-transmission rates and low-energy con-

sumption features [1-5]. Also, it is gaining acceptance in UWB-Internet of Things (UWB-IoT) applications for continuous data-transfer between low-cost sensor devices [6-9]. Due to its low-power emission characteristics, UWB technology is recognized as a viable solution for wireless body area networks (WBANs). This also renders the UWB technology suitable for wearable IoT devices and sensors [5-9].

For UWB systems, several authors have proposed a range of designs for UWB antennas and filters [1-11].

However, not a lot of UWB power dividers have been proposed in the past albeit the fact they are a key component in a variety of microwave systems. For example, power dividers are considered a critical component in the design of balanced mixers [12], phase shifters [13], and feeding networks for phased array antenna (PAA) systems [14-17].

The utilization of 3-port power dividers is particularly critical for the UWB-PAA systems [15-17] that make use of power splitters, for example, a corporate or parallel power splitting system. The corporate feeding network maintains equal path lengths between input and output ports while dividing power between n -output ports with a specific distribution. In situations where 3-port power dividers are frequently utilized, they can be implemented with an n -way power dividing network. The flexible configuration of the two-way power divider enables the employment of numerous stepped sections to produce power divisions with wideband operation capacity [12]. Although utilizing high-isolation power dividers minimizes the reliance on load matching, the operational bandwidth of the power divider network is principally constrained due to the matching required for the radiating elements [12].

The Wilkinson power divider (WPD) [12, 18], also known as the Wilkinson splitter, is a 3-port power divider network that was first introduced in 1960 by Ernest Wilkinson [18]. It has been extensively used in various microwave applications, including wireless communication, PAA, and radar systems. A WPD is a passive splitter that takes one input signal and divides it into n output signals with equal phases and amplitudes. Theoretically, WPD exhibits complete isolation among the output ports at the desired frequency. It is based on the principle of impedance transformation, which is achieved by using quarter-wave transmission-lines (TLs).

The WPD is a type of hybrid splitter that is fundamentally a narrowband device. Many different researchers [13, 14, 19-24] have implemented numerous techniques to enhance its bandwidth of operation. Some of these bandwidth enhancement techniques involve the addition of segmented structures [19], tapered lines [13], and stubs to each section [14, 20, 21]. Other researchers have proposed the use of defective ground structures of different shapes for this purpose [22, 23].

In [14], the authors present an innovative method for broadening the bandwidth of a power divider utilized in six-port interferometers by incorporating radial stubs within a conventional Wilkinson design. Their work across the 3.1-10.6 GHz UWB frequency band reveals a significant enhancement, showcasing a simulated bandwidth expansion of 37.5%. Yu et al. [19] introduce a novel broadband WPD topology utilizing a segmented structure, employing TL segments with shunt capacitors and series resistor-capacitor networks. The design reported in [20] presents a modified approach to the traditional two-section WPD by incorporating open stubs on each branch, demonstrating improved

performance within the UWB frequency band. This design not only outperforms the traditional three-section power divider but also offers a 10% reduction in size and eliminates the need for one resistor, showcasing promising simulation and measurement results. Similarly, Dardeer et al. [21] introduced a cost-effective and compact microstrip-based WPD within the UWB range. The design uses two open-stubs to enhance the bandwidth. Peng et al. [24] demonstrated a UWB non-coplanar power divider design by adding two slots, a tapered and a fan-shaped slot, to enhance the power divider's overall performance.

In this paper, the authors present a study on the design, fabrication, and characterization of a compact and miniaturized UWB 4-Way WPD based on delta-stub with enhanced isolation for UWB-IoT and next-generation wireless system applications. The agreement between the simulated and measured results suggests that the proposed UWB WPD performs well and can be used in UWB-IoT and next-generation wireless systems.

The following sections are organized as follows: Section 2 briefly describes the conventional configuration of the WPD. Section 3 discusses the step-by-step design process of the proposed WPD geometry and its dimensions. Section 4 summarizes the WPD fabrication, characterization, and comparison of simulated and measured results in terms of parameters such as return-loss, insertion-loss, and isolation-loss. Additionally, it provides a comparative study between the design presented in this paper and the existing designs proposed by other researchers. Finally, Section 5 draws conclusions.

2. WPD CONVENTIONAL DESIGN

The WPD functions as a 3-port system, which is typically lossless in nature. When the output ports of a WPD are appropriately matched, the network becomes lossless with only the dissipation of the reflected power. The input power can be divided into two or maybe more in-phase signals of equal amplitude. A quarter-wave ($\lambda/4$) transformer with a characteristic impedance of $\sqrt{2}Z_0$ can be used to realize a 2-way WPD. Fig. 1(a-b), depicts the fundamental two-way design of the WPD. [12-13].

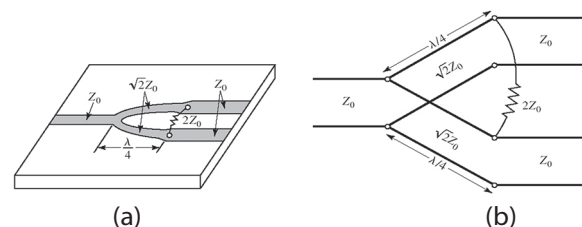


Fig. 1: (a) An equal-split WPD showing the line-impedances and $\lambda/4$ transformers (b) WPD equivalent transmission-line circuit [12]

The initial dimensions of the WPD can be calculated using the well-known transmission-line model [12], as discussed in Eq. (1)-(6), respectively.

The effective dielectric constant (ϵ_{reff}) calculation in Eq. (1) leads to accurate modeling of the microstrip-line, and it depends upon the substrate thickness (h), relative permittivity (ϵ_r), and the conductor width (W).

$$\epsilon_{reff} = \frac{(\epsilon_r + 1)}{2} + \frac{(\epsilon_r - 1)}{2} \left(1 + 12 \frac{h}{W}\right)^{-\frac{1}{2}} \quad (1)$$

Eq. (2) is used to calculate the microstrip-line wavelength (λ in mm), which is correlated with the phase velocity. Where, f is the desired operating frequency. The center frequency is selected as 5.5GHz. It is important to note that Eq. (2) leads to the calculation of the guided wavelength factor, as it is used to determine the size of components such as stubs and the WPD itself at the intended frequency.

$$\lambda = \frac{300}{f \sqrt{\epsilon_{reff}}} \quad (2)$$

The characteristic impedance ($Z_0=50\Omega$) of a microstrip-line is computed using the dimensions from Eq. (3)-(4). The characteristic impedance is a crucial parameter for ensuring impedance matching. The width-to-height ratio (W/h) can be determined by using Eq. (5)-(6), respectively.

$$A = \frac{Z_0}{60} \left(\frac{\epsilon_r + 1}{2}\right)^{1/2} + \frac{\epsilon_r - 1}{\epsilon_r + 1} \left(0.23 + \frac{0.11}{\epsilon_r}\right) \quad (3)$$

$$B = \frac{60\pi^2}{Z_0 \sqrt{\epsilon_r}} \quad (4)$$

For $A > 1.52$:

$$W/h = \frac{8 \exp(A)}{\exp(2A) - 2} \quad (5)$$

For $A < 1.52$:

$$\frac{W}{h} = \frac{2}{\pi} \{B - 1 - \ln(2B - 1)\} + \frac{\epsilon_r - 1}{2\epsilon_r} \left[\ln(B - 1) + 0.39 - \frac{0.61}{\epsilon_r} \right] \quad (6)$$

It is important to note that the parameters in Eq. (3)-(4) are intermediate variables (A and B) that depend on Z_0 . The initially achieved dimensions from the transmission-line model Eq. (1)-(6) are now used to simulate and optimize the WPD design using the CST microwave studio.

3. WPD PROPOSED DESIGN

Fig. 2(a-b) depicts the proposed design for the 1-to-4-way WPD based on delta-stub. The equivalent transmission-line circuit of the proposed WPD is shown in Fig. 2(c). Two delta-stubs, measuring 2.38×0.74 mm (length \times width), are added on both sides of the $\lambda/4$ transformers to improve impedance matching and widen the bandwidth characteristics of the WPD. The labeling of WPD is shown in Fig. 2(a), and the optimum dimension of WPD is shown in Fig. 2(b). For ease of understanding, in the rest of the paper, Port-1 will be referred to as the input-port, whereas Ports 2-5 will be considered output ports,

respectively. The impedance of the input and output ports is approximately 50Ω . The characteristic impedance of the first TLs is $Z_1 = \sqrt{2}Z_0 = 70.7\Omega$.

In the proposed design, at each output port, the power is $1/4^{\text{th}}$ the power of the input-port. So, the transmission loss should be -6dB at each of the output ports. The proposed power divider is designed using an FR4-substrate with a thickness of 0.76mm and ϵ_r of 4.3 , respectively. The FR4 substrate is used in this study because it is a readily available and cost-effective material for the proposed power divider design. Moreover, FR4 adheres to cost limitations in practical applications, particularly in IoT, and facilitates manufacturing and scalability [25]. The FR4 substrate size of 44×24 mm is taken in this study. The 50Ω TL width is taken as 1.5mm , and the length ($\lambda_g/4$) and width of 70.7Ω TL are taken as 7.17mm and 0.65 mm, respectively. The current design uses the delta-stub for better impedance matching and wide bandwidth characteristics. Table 1 lists the modified WPD's optimized dimensions.

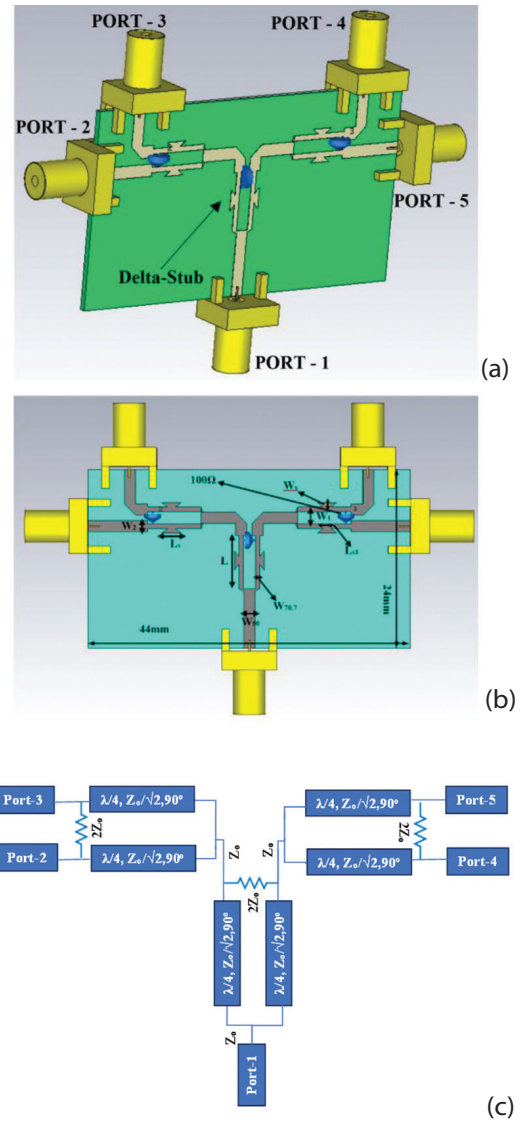


Fig. 2. CST simulation layout of the 1-to-4 way modified WPD (a) Port labeling (b) Optimized dimensions (c) Equivalent transmission-line circuit

Table 1. Parameters of modified 1-to-4 way WPD

W_{50} (mm)	$W_{70.7}$ (mm)	W_1 (mm)	W_2 (mm)
1.5	0.65	1.6	0.75
L (mm)	L_s (mm)	L_{s1} (mm)	W_s (mm)
7.17	2.62	1.1	0.6

4. WPD RESULT AND RELATED DISCUSSION

This section summarizes and validates the results of the proposed and designed WPD working in the UWB frequency range of 3-8GHz. The fabricated prototype of 1-to-4 way modified WPD is shown in Fig. 3. It was fabricated on FR4 substrate ($\epsilon_r = 4.3$, $h = 0.76$ mm, and loss-tangent ($\tan \delta$) of 0.019). The overall dimension of the fabricated prototype was 44 mm \times 24 mm (1056 mm²), as shown in Fig. 3, which demonstrates an 84% size reduction compared to the conventional TL-based WPD with the same frequency band [26]. The prototype of the proposed WPD was measured using Keysight Technologies FieldFox N9916B vector network analyzer (VNA), and the results are discussed in the following sections.

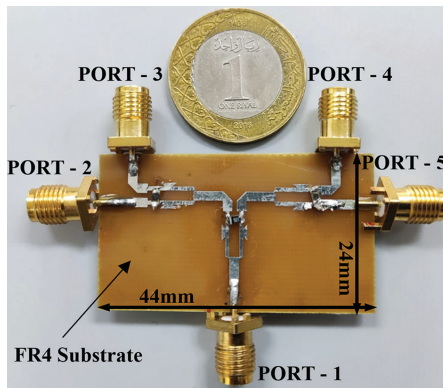


Fig. 3. Fabricated prototype of Proposed WPD

4.1. RETURN-LOSS

Fig. 4 shows the simulated and measured return-loss (S-parameter) results for all the ports of the designed WPD. The Port-1 of the WPD was connected to the Port-1 of the VNA using a high-frequency RF cable and connector to measure the return-loss of WPD. The remaining ports of WPD were terminated using 50 Ω terminators. Fig. 4 shows the simulated and measured return-loss performance across the 3-8GHz frequency band with a magnitude better than -10dB.

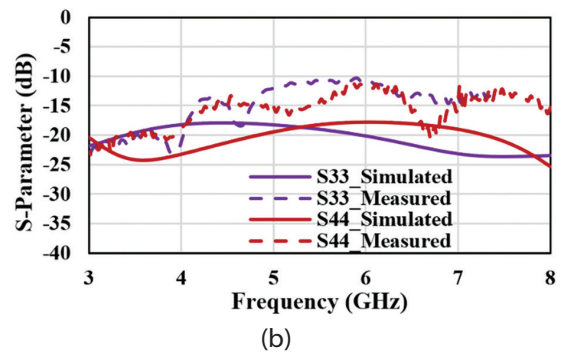
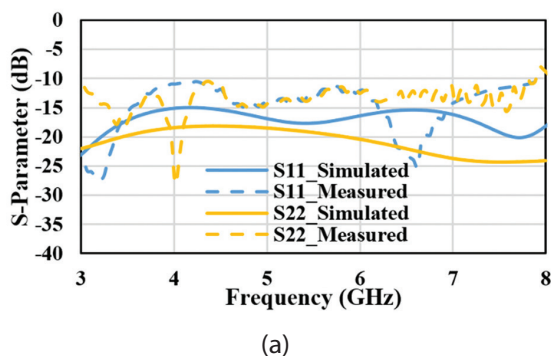


Fig. 4. Simulated and measured return-loss (a) S_{11}, S_{22} (b) S_{33}, S_{44}

4.2. INSERTION-LOSS

For the measurement of WPD insertion-loss, Port-1 of VNA was connected to the WPD Port-1, and Port-2 was connected to the WPD Port-2; meanwhile, WPD Port-3, Port-4, and Port-5 were terminated with 50 Ω terminators. The simulated and measured insertion-loss results for the designed WPD for Port-2 to Port-5 with respect to the input Port-1 are shown in Fig. 5 (a-b).

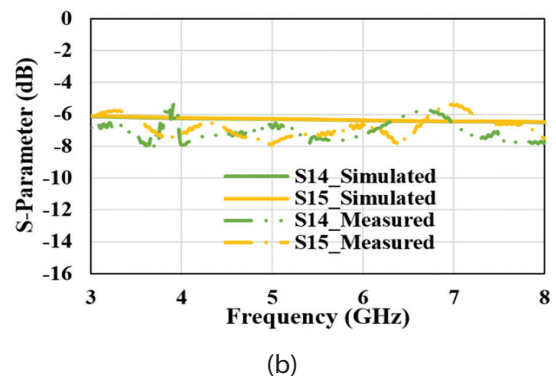
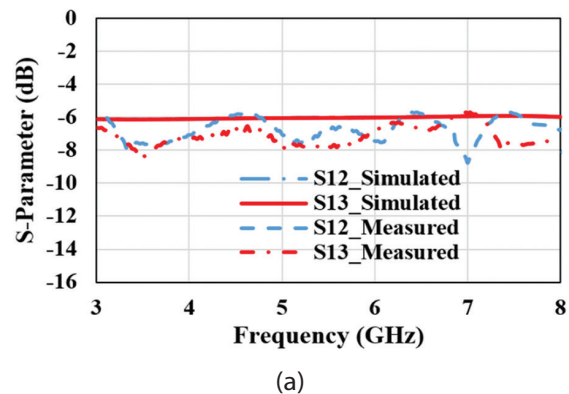


Fig. 5. Simulated and measured insertion-loss (a) S_{12}, S_{13} (b) S_{14}, S_{15}

The simulated and measured insertion-loss shows the value of -6 ± 0.2 dB and -6 ± 2 dB across the UWB frequency range of 3-8 GHz. Fig. 5 also shows the S_{12} results, which highly resemble S_{13}, S_{14} , and S_{15} results, respectively. This means that the input power (from WPD Port-1) has been split equally to all output ports (Port-2 to Port-5), and it performs well with minimal insertion-loss over the specified frequency range.

4.3. ISOLATION-LOSS

Fig. 6(a) shows the simulated and measured isolation-loss results of the designed WPD for Port-3 to Port-5 with respect to the input Port-2. As shown in Fig. 6 (a), the input power was distributed equally to all the power divider's output ports. The isolation-loss is below -10 dB, and it performs well across the required UWB frequency range of 3-8GHz.

Similarly, the simulated and measured isolation-loss results for the designed WPD for Port-4 to Port-3 and Port-5 to Port-3 are shown in Fig. 6(b). The results show excellent isolation between the ports over the frequency range of 3-8GHz. Fig. 6(c) shows the simulated and measured isolation-loss results for the designed WPD for port-5 to port-4 with an isolation-loss below -10dB across the frequency range of 3-8GHz.

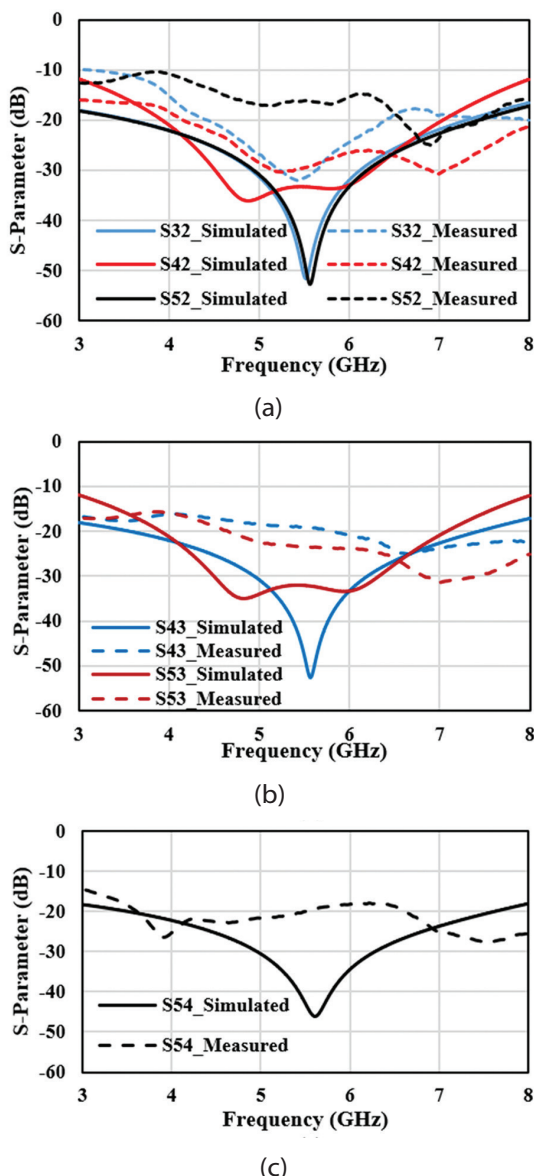


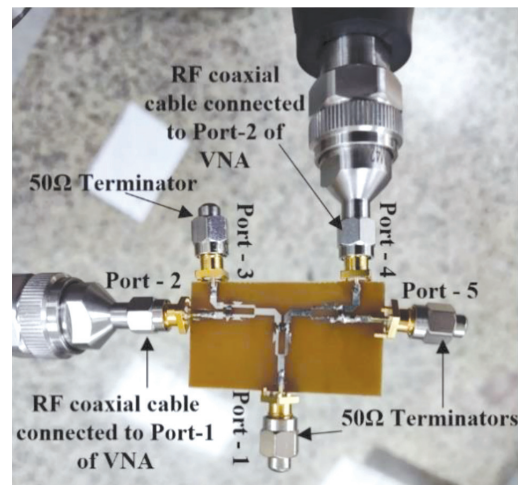
Fig. 6. Simulated and measured Isolation-loss (a) S_{32} , S_{42} , and S_{52} , (b) S_{43} , S_{53} (c) S_{54}

Fig. 7(a-b) shows the overall measurement setup of the WPD. Fig. 7(a) shows that the Port-2 and Port-5

of the device-under-test (DUT) are connected to VNA Port-1 and Port-2, respectively. For WPD isolation-loss measurement, VNA Port-1 was connected to the WPD Port-2, and VNA Port-2 was connected to the WPD Port-4; meanwhile, WPD Port-1, Port-3, and Port-5 were terminated using 50Ω terminators.



(a)



(b)

Fig. 7. Shows the WPD measurements setup using Keysight Technologies FieldFox N9916B Two-Ports vector network analyzer (VNA) and 50Ω Terminators (a) S_{25} measurement setup showing the DUT connected to Keysight VNA (b) Zoom-in on the S_{24} measurement setup

The results presented in Fig. 4 (a-b) and Fig. 5 (a-b) show a slight deviation between the simulated and measured responses of the WPD. The reason for this deviation is the lossy nature of the FR4 substrate, which has the loss-tangent ($\tan \delta$) in the range of 0.019-0.025. Due to the lossy nature of the FR4 substrate, it is very difficult to get the measurement responses exactly the same as the simulated ones. However, it is important

to note that the shape of the simulated and measured S -parameter results is almost similar. This discrepancy can be improved by using high-end Roger's substrates. Another reason for this shift can be due to the amount of solder on the feed-line of the WPD. This problem can be solved in the future by employing precision soldering techniques.

4.4. COMPARATIVE STUDY

The performance of the proposed and designed WPD presented in this paper is compared with previous design works [27-37] and is summarized in Table 2. The designed

WPD has an overall area of $44 \text{ mm} \times 24 \text{ mm} = 1056 \text{ mm}^2$. In contrast, the previous design work [27] occupies an area of $86 \text{ mm} \times 42 \text{ mm} = 3612 \text{ mm}^2$. This comparison shows that the proposed power divider occupies only 29% of the area compared to the design in [27]. This significant size reduction is achieved without any degradation in performance. The data in Table 2 suggest that the proposed design has excellent performance in terms of size reduction, bandwidth, return-loss, insertion-loss, and isolation-loss compared to previous designs. Although the article [28] shows better size reduction, its bandwidth is less compared to the proposed design.

Table 2. Performance comparison of the proposed 1-to-4-way WPD with existing designs

Ref.	Bandwidth (GHz)	Return-loss (dB) (S_{11})	Insertion-loss (dB) (S_{21})	Isolation-loss (dB) (S_{32})	No. of Ports	Technique	Size (mm × mm)	Analysis
[27]	1-4	<-25	6 ± 1.5	<-28	4	Stub	$1.43 \lambda_g \times 0.7 \lambda_g$	High Isolation, Large Size
[28]	2.3-4.4	<-15	0.5	<-17	4	Microstrip-line Marchand balun	$0.4 \lambda_g \times 0.56 \lambda_g$	High Isolation, Low Insertion-loss
[29]	1.08-1.93	<-15	-6.8	<-13	4	Looped Coupled-Line Structures	$0.32 \lambda_g \times 0.32 \lambda_g$	Narrow Bandwidth
[30]	0.54-1.08	<-15	0.3	<-15	4	Meandered Line	$0.27 \lambda_g \times 0.26 \lambda_g$	Narrow Bandwidth, Better Return-loss
[31]	3.1-10	<-10	-6.5	<-13	4	Defected Ground Structure	$1.97 \lambda_g \times 2.5 \lambda_g$	Wide Bandwidth, Large size
[32]	1.6-2.6	<-16	-7	<-20	4	Coshared Multi-Mode Resonators	$0.63 \lambda_g \times 0.33 \lambda_g$	Narrow Bandwidth, Better Isolation
[33]	1.08-1.93	<-15	-6	<-13	4	Looped Coupled-Line Structures	$0.5 \lambda_g \times 0.5 \lambda_g$	Narrow Bandwidth
[34]	0.83-1.39	<-10	-	<-12	4	Coupled-Lines	$0.55 \lambda_g \times 0.16 \lambda_g$	Narrow Bandwidth, Compact Size
[35]	8.6-12.2	<-15	-7.8	-	4	Substrate Integrated waveguide method	$4 \lambda_g \times 4 \lambda_g$	Wide Bandwidth, Large Size
[36]	7.92-9.53	<-28	0.37	<-20	4	Suspended Stripline power divider	$0.8 \lambda_g \times 0.6 \lambda_g$	Narrow Bandwidth, Low Insertion-loss, Better Return, and Isolation losses
[37]	17-19	<-12.5	2.25	<-20	4	Gysel Power Divider	$3.29 \lambda_g \times 0.8 \lambda_g$	Large Size
[This Work]	3-8	<-10	6 ± 1	<-10	4	Delta-Stub	$0.9 \lambda_g \times 0.5 \lambda_g$	Wide Bandwidth, Good Insertion and Return losses, Compact Size

The proposed WPD covers a moderate bandwidth of 3-8 GHz, making it suitable for UWB applications. In comparison, references [31] and [35] offer wide bandwidths but at the expense of significantly large sizes, while most other references cover narrow bandwidths, limiting their applicability in UWB systems. The return-loss achieved in this work is <-10 dB, which is acceptable for many applications. In contrast, references [30] and [36] demonstrate better return-loss performance (<-20 dB and <-28 dB, respectively), although they either have a much narrower bandwidth or a slightly larger size. The insertion-loss in the proposed design is approximately 6 ± 1 dB, comparable to most other references. Articles [28] and [36] have significantly lower insertion-loss but come with other trade-offs, such as isolation or application bandwidth.

In terms of isolation-loss, the proposed design demonstrates <-10 dB, which is decent but not as high as some

other researchers [27], [32], and [36]. The designs presented in [27] has larger size, while [32] and [36] offer better isolation-loss but narrow bandwidth, making them more suitable for applications requiring high isolation.

Additionally, the proposed design presented in this work is relatively compact compared to most of the designs discussed in Table 2. A comparable compact design is presented in [34], but it does not offer the same bandwidth or performance metrics.

Articles [35-37] are based on substrate integrated, Gysel, and suspended-stripline power dividers. These articles present designs with lesser bandwidth and larger sizes compared to the proposed design. Furthermore, the proposed design's fabrication process is much easier compared to these works, as the latter uses multilayer techniques that increase fabrication cost and complexity. This highlights the advantage of the single-layer WPD method proposed in this paper.

Overall, the proposed work offers a balanced approach with moderate bandwidth, good return-loss, and insertion-loss, along with a compact size. The unique use of delta-stubs enhances operational bandwidth and impedance-matching characteristics, setting this design apart from other techniques. The specific focus on next-generation UWB-IoT antenna array systems highlights the practical applicability of this design in modern technologies.

5. CONCLUSION

In this study, we have designed, fabricated, and characterized a unique 1-to-4 way WPD employing the delta-stub technique for a wideband frequency range operation between 3-8 GHz. This study demonstrates that the proposed WPD outperforms previous designs by offering a smaller size, which leads to lower fabrication costs in practical applications. The proposed compact and wideband power divider has exhibited good performance with an overall size reduction of 71% as compared to previous work [27] by using stubs.

The compact yet wideband characteristics of the proposed WPD have yielded robust performance attributes, including equal power distribution, low insertion-loss, improved isolation, and adequate return losses across all ports. The unique use of delta-stubs enhances operational bandwidth and impedance-matching characteristics, setting this design apart from other techniques. These results indicate that the proposed WPD is an appropriate candidate for integration into UWB-IoT antenna array feeding networks and emerging next-generation wireless systems.

In the future, we plan to integrate the currently presented 1-to-4 way WPD with a similar metamaterial-based beamforming network and antennas [1, 3, 16] for real-world testing and implementation of such systems for 5G and next-generation wireless systems. This integration aims to explore further enhancements in beamforming capabilities and dynamic beam-shaping functionalities.

6. REFERENCES

- [1] G. Adamiuk, T. Zwick, W. Wiesbeck, "UWB Antennas for Communication Systems", *Proceedings of the IEEE*, Vol. 100, No. 7, 2012, pp. 2308-2321.
- [2] Z. G. Wang, R. You, M. Yang, J. Zhou, M. Wang, "Design of a Monopole Antenna for Wifi-UWB Based on Characteristic Mode Theory", *Progress in Electromagnetics Research M*, Vol. 125, 2024, pp. 107-116.
- [3] A. K. Vallappil, B. A. Khawaja, M. K. A. Rahim, M. N. Iqbal, H. T. Chattha, M. F. B. Mohamad Ali, "A Compact Triple-Band UWB Inverted Triangular Antenna with Dual-Notch Band Characteristics Using SSRR Metamaterial Structure for Use in Next-Generation Wireless Systems", *Fractal and Fractional*, Vol. 6, No. 8, 2022, p. 422.
- [4] K. Shafique, B. A. Khawaja, M. A. Tarar, B. M. Khan, M. Mustaqim, A. Raza, "A Wearable Ultra-Wideband Antenna for Wireless Body Area Networks", *Microwave and Optical Technology Letters*, Vol. 58, No. 7, 2016, pp. 1710-1715.
- [5] J. R. Ojha, M. Peters, "Patch Antennas and Microstrip Lines", *Microwave and Millimeter Wave Technologies Modern UWB Antennas and Equipment*, InTechOpen, 2010, pp. 49-62.
- [6] K. Shafique, B. A. Khawaja, M. D. Khurram, S. M. Sibtain, Y. Siddiqui, M. Mustaqim, H. T. Chattha, X. Yang, "Energy Harvesting Using a Low-Cost Rectenna for Internet of Things (IoT) Applications", *IEEE Access*, Vol. 6, 2018, pp. 30932-30941.
- [7] O. Cetinkaya, O. B. Akan, "Electric-Field Energy Harvesting from Lighting Elements for Battery-Less Internet of Things", *IEEE Access*, Vol. 5, 2017, pp. 7423-7434.
- [8] L. Davoli, L. Belli, A. Cilfone, G. Ferrari, "From Micro to Macro IoT: Challenges and Solutions in The Integration of IEEE 802.15. 4/802.11 And Sub-GHz Technologies", *IEEE Internet of Things Journal*, Vol. 5, No. 2, 2018, pp. 784-793.
- [9] Z. Song et al. "Origami Metamaterials for Ultra-Wideband and Large-Depth Reflection Modulation", *Nature Communications*, Vol. 15, 2024, p. 3181.
- [10] C.-H. Kang, S.-J. Wu, J.-H. Tarng, "A Novel Folded UWB Antenna for Wireless Body Area Network", *IEEE Transactions on Antennas and Propagation*, Vol. 60, No. 2, 2012, pp. 1139-1142.
- [11] S. N. Mahmood, A. J. Ishak, A. Ismail, A. C. Soh, Z. Zakaria, S. Alani, "ON-OFF Body Ultra-Wideband (UWB) Antenna for Wireless Body Area Networks (WBAN): A Review", *IEEE Access*, Vol. 8, 2020, pp. 150844-150863.
- [12] D. M. Pozar, "Microwave Engineering", 4th Edition, John Wiley and Sons, 2011.
- [13] F. Razzaz, S. M. Saeed, M. A. S. Alkanhal, "Compact Ultra-Wideband Wilkinson Power Dividers Using Linearly Tapered Transmission Lines", *Electronics*, Vol. 11, No. 19, 2022, pp. 1-10.

- [14] N. H. A. Rahim, M. F. A. H. Saari, S. Z. Ibrahim, M. S. Razalli, G. S. Tan, "Wideband Power Divider Using Radial Stub for Six-Port Interferometer", *Proceedings of the IEEE Asia-Pacific Conference on Applied Electromagnetics*, Langkawi, Malaysia 11-13 December 2016, pp. 127-131.
- [15] A. K. Vallappil, B. A. Khawaja, M. K. A. Rahim, M. Uzair, M. Jamil, Q. Awais, "Minkowski-Sierpinski Fractal Structure-Inspired 2×2 Antenna Array for Use in Next-Generation Wireless Systems", *Fractal and Fractional*, Vol. 7, No. 2, 2023, pp. 1-18.
- [16] A. K. Vallappil, M. K. A. Rahim, B. A. Khawaja, M. N. Iqbal, "A Miniaturized Metamaterial-Loaded Switched-Beam Antenna Array System with Enhanced Bandwidth for 5G Applications", *IEEE Access*, Vol. 12, 2024, pp. 6684-6697.
- [17] B. Khawaja, "Eight-Port Tapered-Edged Antenna Array with Symmetrical Slots and Reduced Mutual-Coupling for Next-Generation Wireless and Internet of Things (IoT) Applications", *International Journal of Electrical and Computer Engineering Systems*, Vol. 14, No. 6, 2023, pp. 695-702.
- [18] E. J. Wilkinson, "An N-way Power Divider", *IEEE Transactions on Microwave Theory and Techniques*, Vol. 8, No. 1, 1960, pp. 116-118.
- [19] T. Yu, "A Broadband Wilkinson Power Divider Based on the Segmented Structure", *IEEE Transactions on Microwave Theory and Techniques*, Vol. 66, No. 4, 2018, pp. 1902-1911.
- [20] X.-P. Ou, Q.-X. Chu, "A Modified Two-Section UWB Wilkinson Power Divider", *Proceedings of the International Conference on Microwave and Millimeter Wave Technology*, Nanjing, China, 21-24 April 2008, pp. 1258-1260.
- [21] O. Dardeer, T. Abouelnaga, A. Mohra, H. Elhennawy, "Compact UWB Power Divider, Analysis and Design", *Journal of Electromagnetic Analysis and Applications*, Vol. 9, No. 2, 2017, pp. 9-21.
- [22] S. H. Ramazania, S. Chamaani, S. A. Mirtaheri, F. K. M. Yazdi, M. Yazdani, "A UWB 1 to 4 Wilkinson Power Divider with Triple High-Q Band-Notched Characteristic Using U-Shaped DGS", *Proceedings of the IEEE International Conference on Ultra-Wideband*, Syracuse, NY, USA, 17-20 September 2012, pp. 302-305.
- [23] M. Salman, Y. Jang, J. Lim, D. Ahn, S.-M. Han, "Novel Wilkinson Power Divider with an Isolation Resistor on a Defected Ground Structure with Improved Isolation", *Applied Sciences*, Vol. 11, No. 9, 2021, pp. 1-21.
- [24] H. Peng, Z. Yang, Y. Liu, T. Yang, K. Tan, "An Improved UWB Non-Coplanar Power Divider", *Progress in Electromagnetics Research*, Vol. 138, 2013, pp. 31-39.
- [25] P.K. Malik, P.N. Shastry, "Internet of Things Enabled Antennas for Biomedical Devices and Systems: Impact, Challenges and Applications", *Springer Tracts in Electrical and Electronics Engineering*, Springer Singapore, 2023.
- [26] F. A. Shaikh, S. Khan, A. Z. Alam, M. H. Habaebi, O. O. Khalifa, T. A. Khan, "Design And Analysis Of 1-To-4 Wilkinson Power Divider for Antenna Array Feeding Network", *Proceedings of the IEEE International Conference on Innovative Research and Development*, Bangkok, Thailand, 11-12 May 2018, pp. 1-4.
- [27] H. B. Tila et al. "Novel low cost 1-to-4 Microstrip Wilkinson Power Divider", *Proceedings of the IEEE MTT-S International Wireless Symposium*, Shanghai, China, 14-16 March 2016, pp. 1-4.
- [28] K. Song, J. Yao, C. Zhong, S. R. Patience, "Miniaturised Wideband Four-Way Out-Of-Phase Power Divider Based on Marchand Balun", *IET Microwaves, Antennas & Propagation*, Vol. 13, No. 15, 2019, pp. 2682-2686.
- [29] H. Zhu, A. M. Abbosh, L. Guo, "Wideband Four-Way Filtering Power Divider with Sharp Selectivity and Wide Stopband Using Looped Coupled-Line Structures", *IEEE Microwave and Wireless Components Letters*, Vol. 26, No. 6, 2016, pp. 413-415.
- [30] Ö. Kasar, "Design and Implementation of Compact Four Way Wilkinson Power Divider for UHF Applications", *Sigma Journal of Engineering and Natural Sciences*, Vol. 38, No. 4, 2020, pp. 2193-2203
- [31] M. Squartecchia, B. Cimoli, V. Midili, T. K. Johansen, V. Zhurbenko, "Design of a Planar Ultra-Wideband Four-Way Power Divider/Combiner Using Defected Ground Structures", *Proceedings of the 47th European Microwave Conference*, Nuremberg, Germany, 10-12 October 2017, pp. 9-12.

- [32] G. Zhang, Z. Qian, J. Yang, J.-S. Hong, "Wideband Four-Way Filtering Power Divider with Sharp Selectivity and High Isolation Using Coshared Multi-Mode Resonators", *IEEE Microwave and Wireless Components Letters*, Vol. 29, No. 10, 2019, pp. 641-644.
- [33] H. Zhu, A. M. Abbosh, L. Guo, "Wideband Four-Way Filtering Power Divider with Sharp Selectivity and Wide Stopband Using Looped Coupled-Line Structures", *IEEE Microwave and Wireless Components Letters*, Vol. 26, No. 6, 2016, pp. 413-415.
- [34] K. Song, Y. Mo, Y. Fan, "Wideband Four-Way Filtering-Response Power Divider with Improved Output Isolation Based on Coupled Lines", *IEEE Microwave and Wireless Components Letters*, Vol. 24, No. 10, 2014, pp. 674-676.
- [35] X. Zou, C.-M. Tong, D.-W. Yu, "Y-Junction Power Divider Based on Substrate Integrated Waveguide", *Electronics Letters*, Vol. 47, No. 25, 2011, pp. 1375-1376.
- [36] S. Guo, K. Song, Y. Fan, "Compact Four-Way Suspended-Stripline Power Divider with Low Loss and High Isolation", *International Journal of Microwave and Wireless Technologies*, Vol. 12, No. 8, 2020, pp. 749-753.
- [37] H. Chen, W. Che, X. Wang, W. Feng, "Size-Reduced Planar and Nonplanar SIW Gysel Power Divider Based on Low Temperature Co-Fired Ceramic Technology", *IEEE Microwave and Wireless Components Letters*, Vol. 27, No. 12, 2017, pp. 1065-1067.